The Directionality of an Optical Fiber High-Frequency Acoustic Sensor for Partial Discharge Detection and Location

Zhao Zhiqiang, Mark MacAlpine, and M. Süleyman Demokan, *Senior Member, IEEE*

***Abstract*—Fiber-optic acoustic sensors are being developed for the detection and location of partial discharges in oil-filled transformers. The partial discharges can be detected acoustically and located by the triangulation method with the sensors placed inside the transformer tank. In this application, the directionality of the sensor should be as flat as possible within at least $\pm 40^\circ$ from the sensor axis and for a frequency range up to 150 kHz. A calculation of the directionality of a fiber coil acoustic sensor was made using a plane wave approximation. The calculation showed that if the diameter of a fiber coil is less than 20 mm, its directionality is relatively flat within $\pm 40^\circ$ for frequencies lower than 150 kHz.**

The directionality of an optical fiber acoustic sensor for the frequency range of 50–300 kHz was measured experimentally in an oil tank. The effect of reflected waves was avoided by using a gating technique. The experimental results show somewhat different directionality patterns from the theoretical results but are internally consistent and with maxima and minima at frequencies close to those predicted. The discrepancy is believed to be due to a resonance effect which is not taken into account in the theoretical model. However, the sensor achieves the directionality performance required for the application.

***Index Terms*—Acoustic signal detection, acoustooptic measurements, optical fiber transducers, partial discharges.**

I. Introduction

PARTIAL discharges in transformers are an indicator of the condition of the solid insulation as they are localized electrical breakdown of small voids (which should not be present in good insulation). They may be detected electrically as pulses in the supply circuit but this gives no indication of location. A method for locating the partial discharge (pd) sites is provided by locating piezoelectric transducers on the outside of the transformer tank and attempting triangulation. However, this method is vitiated by the different velocities of sound in the solid insulation, in the oil and in the steel of the tank walls, which thus tend to provide multiple routes, and travel times, between source (pd site) and transducer [1].

The advantages of using fiber optic sensors in this application are that the fiber sensor can be placed inside the transformer tank without affecting the insulation integrity, and that fiber optic sensors have intrinsic immunity to electromagnetic interference. By placing the sensor heads inside the tank, instead of mounting them on outside wall of the tank (as with piezoelectric sensors), the above problems arising from the different velocities of sound will be greatly diminished and the accuracy of locating partial discharges by triangulation should be very much improved.

Manuscript received April 12, 1999; revised February 7, 2000. This work was supported by the Hong Kong Polytechnic University under Project 350/263.

The authors are with The Hong Kong Polytechnic University, Kowloon, Hong Kong, China.

Publisher Item Identifier S 0733-8724(00)05071-4.

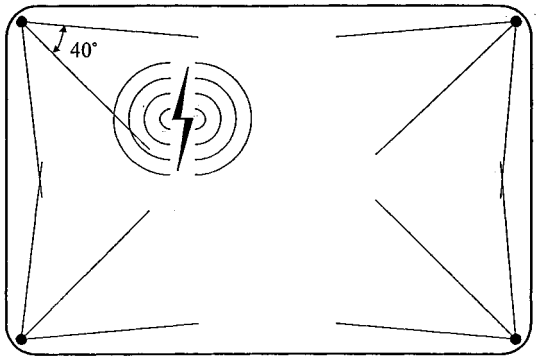

Fig. 1. A transformer tank with four sensors placed inside at its corners.

The frequency range of the sensor needs to be 50–300 kHz, the sensitivity should be at least 0.2 Pa, and the sensor should be able to respond to ultrasonic waves at a wide range of incidence angles for the purpose of locating partial discharges [2], [3]. If we put the sensor heads at the corners of the transformer, as shown in Fig. 1, the response of the sensor should be relatively flat over at least $\pm 40^\circ$ from the normal, to enable efficient triangulation.

The directionality, or directional sensitivity, of a fiber sensor to a sound wave depends on the sound frequency and wavelength, and on the geometric structure of the sensor. For a fiber acoustic sensor configured as a fiber coil, the directionality of the sensor is not isotropic when the sound wavelength is less than the diameter of the coil. The higher the acoustic frequency, the greater the effect of the incidence angle on the response. The velocity of acoustic waves in transformer oil is about 1400 m/s. For a 100-kHz ultrasonic wave, the wavelength is therefore 14 mm, while for 300 kHz the wavelength is only 5 mm. By using a high-NA bend-insensitive fiber, a fiber coil diameter of 10∼20 mm can be realized [4]. The reduction of coil size is limited by the bend loss and by the fact that a long fiber length is needed for high sensitivity.

In this paper, a theoretical calculation of the directionality of a fiber coil acoustic sensor is first presented based on a plane wave approximation. Then, an experiment to measure the directionality of a fiber acoustic sensor is described and the experimental results given. These showed a general agreement with the calculation in terms of the maxima and minima but a much lower

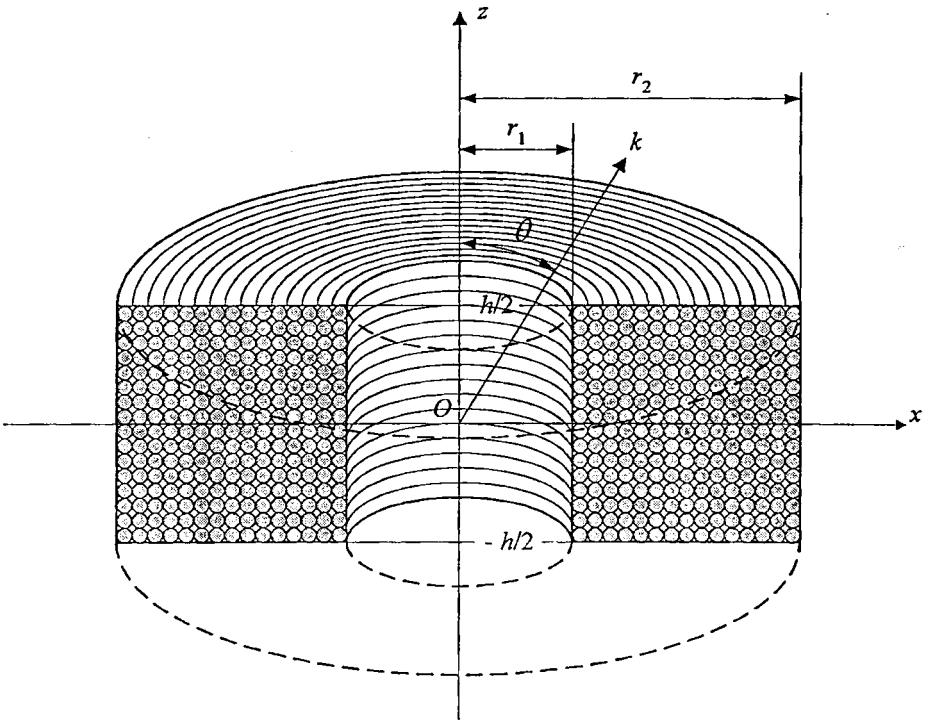

Fig. 2. Geometric structure of the sensing coil (not to scale).

sensitivity than expected for waves incident close to the normal. This effect is discussed and suggestions as to its origin are put forward.

II. Directionality Calculation for a Fiber Coil Acoustic Sensor

In designing the fiber acoustic sensor for partial discharge detection, it is necessary to make a theoretical calculation of the directionality, in order to choose the parameters according to the requirements of the application and to ensure acceptable directionality. In this section, a simplified calculation of the directionality of the fiber coil acoustic sensor is presented.

A. Derivation of the Directionality Expressions Using the Plane-Wave Method

The geometric structure of the sensor is shown in Fig. 2. The fiber is wound layer by layer to form a hollow cylindrical coil with inner radius r_1, outer radius r_2, and height h. The outer diameter of the fiber is d, and the total fiber length is L.

When put into an acoustic field, the fiber will experience a strain according to the variation of the sound pressure and the position of the fiber in the field. When light propagates along the fiber, an additional phase shift will be induced by the strain and by means of the acoustooptic effect. Let this phase shift per unit fiber length be $\Delta\beta(t, l)$, where l is the coordinate along the fiber. The total phase shift induced by sound pressure is

$$\Delta\phi_s(t) = \int_0^L \Delta\beta(t, l)\, dl \tag{1}$$

Because of the time delay of the light propagating through the fiber, the variable t in the right-hand side of (1) should be replaced by $t - l/v_o$, where v_o is the effective light velocity in the fiber. Thus

$$\Delta\phi_s(t) = \int_0^L \Delta\beta\left(t - \frac{l}{v_o}, l\right) dl. \tag{2}$$

The induced acoustooptic perturbation depends on the local strain in the fiber coil. An accurate analysis of this strain, considering the composite medium of glass fiber, coating and encapsulating material, as well as reflections from the boundaries, is a complicated. Here, we adopt the approximation method used by Knudsen and Bløtekjær [5], in which, an incident plane wave with its direction of propagation inclined at an angle θ with the coil axis (z-axis) is considered, and the induced acousto-optic perturbation is taken to be proportional to the amplitude of the sound field at every point. Reflections at the transducer boundaries and effects due to the composite structure are neglected. The perturbation due to a plane wave can be written as

$$\Delta\beta(t, \Omega, \vec{K}) = \delta\beta_0 \exp[i(\Omega t - Kr\cos\varphi\sin\theta - Kz\cos\theta)] \tag{3}$$

where

- $\delta\beta_0$ peak amplitude of the perturbation and is proportional to the acoustic pressure field;
- Ω and K acoustic angular frequency and the amplitude of wave vector, respectively;
- r, φ, and z cylindrical coordinates.

By substituting (3) into (2), and assuming that l is approximately constant in one turn of fiber, we have the contribution of one turn of fiber to the $\Delta\phi_s$ as

$$\begin{aligned}\Delta\phi_{s,\,\mathrm{turn}}(t,\,\Omega,\,\vec{K}) &= \int_0^{2\pi} \delta\beta_0 \exp\left\{ i\left[\Omega\left(t-\frac{l}{v_o}\right) - Kr\cos\varphi\sin\theta - Kz\cos\theta\right]\right\} r\,d\varphi \\ &= \delta\beta_0 \exp\left[i\Omega\left(t-\frac{l}{v_o}\right)\right]\exp(-iKz\cos\theta) r \cdot \int_0^{2\pi}\exp(-iKr\sin\theta\cos\varphi)\,d\varphi\end{aligned}$$

The integral in the right-hand side of the above equation is equal to $2\pi J_0(Kr\sin\theta)$, where $J_0(x)$ is the zero-order Bessel function of the first kind. Thus

$$\begin{aligned}\Delta\phi_{s,\,\mathrm{turn}}(t,\,\Omega,\,\vec{K}) &= \delta\beta_0 2\pi \exp\left[i\Omega\left(t-\frac{l}{v_o}\right)\right] \cdot \exp(-iKz\cos\theta) r\,J_0(Kr\sin\theta). \end{aligned} \tag{4}$$

The contribution of one layer of fiber to the $\Delta\phi_s$ is the sum of the contribution of M turns, where M is the number of turns in one layer. Approximating the sum by an integral and assuming also that l is approximately constant within one layer,

$$\begin{aligned}\Delta\phi_{s,\,\mathrm{layer}}(t,\,\Omega,\,\vec{K}) &\approx \frac{1}{d}\int_{-(h/2)}^{(h/2)} \Delta\phi_{s,\,\mathrm{turn}}(t,\,\Omega,\,\vec{K})\,dz \\ &= \delta\beta_0\frac{4\pi}{dK\cos\theta}\exp\left[i\Omega\left(t-\frac{l}{v_o}\right)\right] r \cdot J_0(Kr\sin\theta)\sin\left(\frac{Kh\cos\theta}{2}\right).\end{aligned} \tag{5}$$

The integral in (2) may be evaluated by integrating over the cylinder radius from r_1 to r_2

$$\begin{aligned}\Delta\phi_s(t,\,\Omega,\,\vec{K}) &= \frac{1}{d}\int_{r_1}^{r_2}\Delta\phi_{s,\,\mathrm{layer}}(t,\,\Omega,\,K)\,dr \\ &= \delta\beta_0\frac{4\pi}{d^2K\cos\theta}\sin\left(\frac{Kh\cos\theta}{2}\right)\exp(i\Omega t) \cdot \int_{r_1}^{r_2}\exp\left(-i\Omega\frac{l}{v_o}\right) r\,J_0(Kr\sin\theta)\,dr.\end{aligned} \tag{6}$$

In this evaluation, the fiber length coordinate l needs to be expressed approximately as a function of r:

$$l(r) = \frac{h}{d}\int_{r_1}^{r}\frac{2\pi r}{d}\,dr = \frac{\pi h}{d^2}(r^2 - r_1^2). \tag{7}$$

Substituting (7) into (6), we have

$$\begin{aligned}\Delta\phi_s(t,\,\Omega,\,\vec{K}) &= \delta\beta_0\frac{4\pi}{d^2K\cos\theta}\sin\left(\frac{Kh\cos\theta}{2}\right)\exp(i\Omega t) \cdot \int_{r_1}^{r_2}\exp\left[-i\frac{\pi\Omega h}{v_o d^2}(r^2-r_1^2)\right] r\,J_0(Kr\sin\theta)\,dr.\end{aligned} \tag{8}$$

The integral in the right-hand side of (8) does not have an analytical solution, except when the acoustic wave is incident parallel to the z-axis (i.e., $\theta = 0$). In this case, $J_0(Kr\sin\theta) = 1$, and (8) reduces to

$$\begin{aligned}\Delta\phi_{s0}(t,\,\Omega,\,K) &= \delta\beta_0\frac{4v_o}{\Omega hK}\sin\left(\frac{Kh}{2}\right)\sin\left(\frac{\Omega L}{2v_o}\right) \cdot \exp\left[i\Omega\left(t-\frac{L}{2v_o}\right)\right]\end{aligned} \tag{9}$$

where

$$L = \frac{\pi h}{d^2}(r_2^2 - r_1^2). \tag{10}$$

Substituting $K = \Omega/v_a$ into (9), where v_a is the velocity of sound in the composite fiber material

$$|\Delta\phi_{s0}| = \delta\beta_0\frac{4v_o v_a}{h\Omega^2}\sin\left(\frac{\Omega h}{2v_a}\right)\sin\left(\frac{\Omega L}{2v_o}\right) \tag{11}$$

or

$$|\Delta\phi_{s0}| = \delta\beta_0\frac{2v_o}{\Omega}\cdot\frac{\sin\left(\dfrac{\Omega h}{2v_a}\right)}{\dfrac{\Omega h}{2v_a}}\cdot\sin\left(\frac{\Omega L}{2v_o}\right). \tag{12}$$

It can be seen from (12) that $|\Delta\phi_{s0}|$ is at its maximum when $h = 0$ and when $L = \pi v_o/\Omega$. Thus, that for a given fiber length L, a planar coil has maximum acoustic sensitivity in its normal direction. However, for a given L, a planar coil will have the largest outer diameter, so it will have the narrowest directionality. For a flat directionality, h must be a compromise. If h is half the wavelength of sound, Λ, where $\Lambda = 2\pi v_a/\Omega$, $|\Delta\phi_{s0}|$ is 0.64 of the maximum value at $h = 0$. This means that for a given coil height h, the acoustic sensitivity in the normal direction of the coil is not simply proportional to the fiber length L, but has a maximum at $L_M = \pi v_o/\Omega$. For values of L greater than L_M, the sensitivity will decrease with increasing L. This is because of the finite propagating velocity of light in the fiber. When $L \ll L_M$, the sensitivity in the normal direction is approximately proportional to the fiber length for a given h. The typical values of v_o and v_a are 2.05×10^8 and 2300 m/s, respectively, [5]. If we consider a 100-kHz ultrasonic wave, then $L_M = 1025$ m, which is much longer than a practical length of sensing fiber. Therefore, in the relevant frequency range and for a fiber length of ~100 m or less and for a given coil height ~~h~~, the sensitivity in the normal direction is virtually proportional to the fiber length.

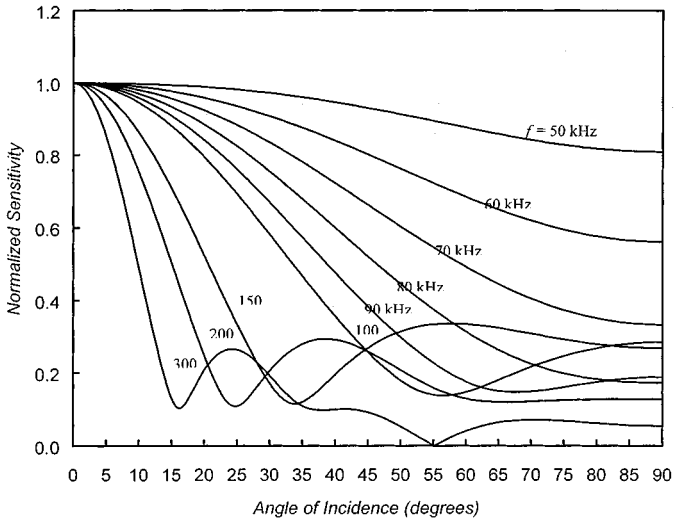

Fig. 3. Normalized directional sensitivities at various frequencies, the effect of the finite velocity of light in the fiber being considered. $r_1 = 5$ mm, $r_2 = 15$ mm, $h = (1/2)\Lambda$.

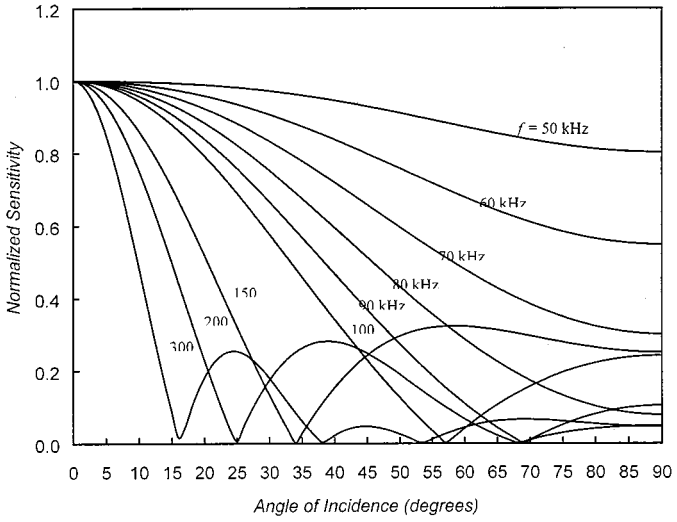

Fig. 4. Normalized directional sensitivities at various frequencies, the effect of the finite velocity of light in the fiber not being considered. $r_1 = 5$ mm, $r_2 = 15$ mm, $h = (1/2)\Lambda$.

In calculating the directionality the time-varying amplitude of $\Delta\phi_s$ is not needed, so, from (8),

$$|\Delta\phi_s| = \delta\beta_0 \frac{4\pi}{d^2 K\cos\theta}\sin\left(\frac{Kh\cos\theta}{2}\right)\cdot[S_1^2+S_2^2]^{1/2} \quad (13)$$

where

$$S_1 = \int_{r_1}^{r_2} \cos\left[\frac{\pi\Omega h}{v_o d^2}(r^2-r_1^2)\right] r\,J_0(Kr\sin\theta)\,dr \quad (14)$$

$$S_2 = \int_{r_1}^{r_2} \sin\left[\frac{\pi\Omega h}{v_o d^2}(r^2-r_1^2)\right] r\,J_0(Kr\sin\theta)\,dr. \quad (15)$$

In (6), if $\Omega l/v_o \ll 1$, $\exp(-i\Omega l/v_o)$ will be approximately equal to 1, then the integral can become simpler with $\exp(-i\Omega l/v_o) = 1$. By doing this the effect of the time delay as the light wave propagates along the fiber is neglected. For example, if $\Omega = 2\pi f_a = 2\pi \times 100$ kHz, $l \approx 100$ m, $v_o = 2.05 \times 10^8$ then $\Omega l/v_o = 0.306$. So, neglecting the time delay would introduce an inaccuracy.

B. Numerical Calculations and Explanations of the Results

The numerical calculation of (12)–(15) was made by a FORTRAN program. The results for different frequencies and fiber coil parameters are shown graphically in Figs. 3–8. The fiber outer diameter was taken as 140 μm, which is close to that of one of the high-NA sensing fibers. The inner diameter of the coil was taken as $r_1 = 5$ mm, which is acceptable when considering the bending loss for high-NA sensing fibers [4]. The velocity of sound in the material was again taken as $v_a = 2300$ m/s.

In Fig. 3, the outer diameter of the fiber coil was fixed as $r_2 = 15$ mm, and the height of the cylinder was taken as a half of the sound wavelength, which is changed with the sound frequency. The curves show the relative response with the maximum ($\theta = 0$) normalized to unity. It can be seen from the curves that the directionality is relatively flat for small f but narrow and variable for large f.

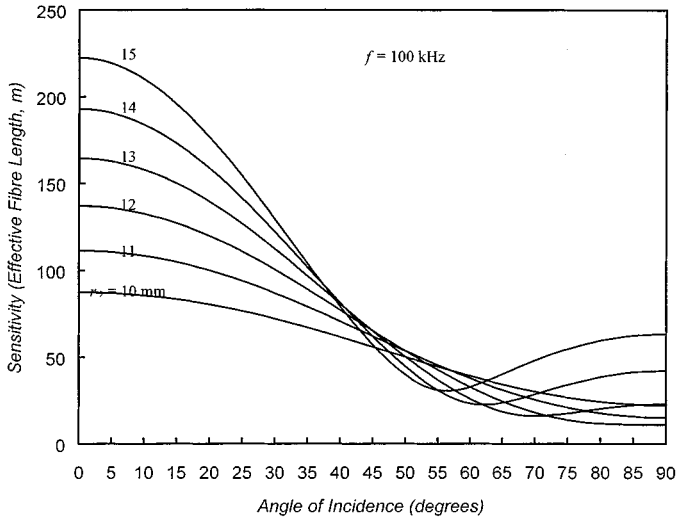

Fig. 5. Directional sensitivities for various coil outer diameters, with $r_1 = 5$ mm, $f = 100$ kHz, $h = (1/2)\Lambda = 11.5$ mm.

For a comparison, the curves with the same parameters as in Fig. 3 but using the simplified formula, that is, neglecting the exponential factor in the integral of (6), are calculated and shown in Fig. 4. It can be seen from Figs. 3 and 4 that the inaccuracy of the simplified model is negligible for lower frequencies and small angles of incidence, but is not negligible when the frequency is high and the incidence angle is large.

Figs. 5 and 6 are for various coil outer diameters from 10 mm through 15 mm, and sound frequencies of 100 and 150 kHz, respectively. The height of the cylinder is also taken as a half of the sound wavelength Λ. Because the height of coil h is kept constant (equal to $\Lambda/2$) for the curves at each frequency f_a in these two figures, and r_1 is the same for all of them, a larger r_2 corresponds to a longer fiber length in the coil. Therefore, the response is higher for a larger r_2 in each of these two figures.

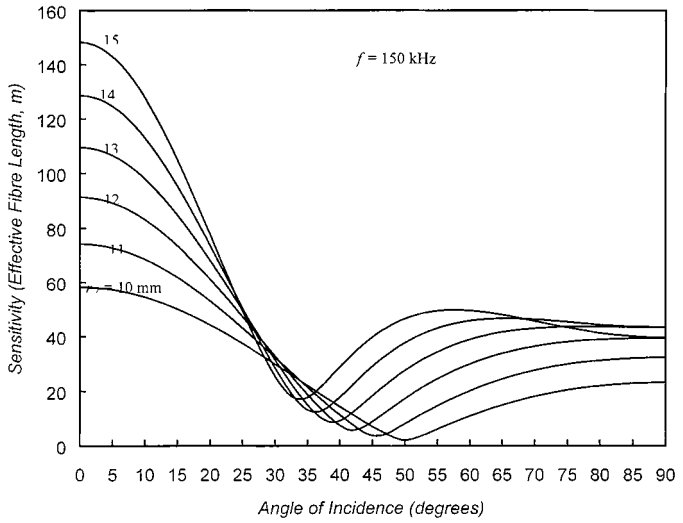

Fig. 6. Directional sensitivities for various coil outer diameters, with $r_1 = 5$ mm, $f = 150$ kHz, $h = (1/2)\Lambda = 11.5$ mm.

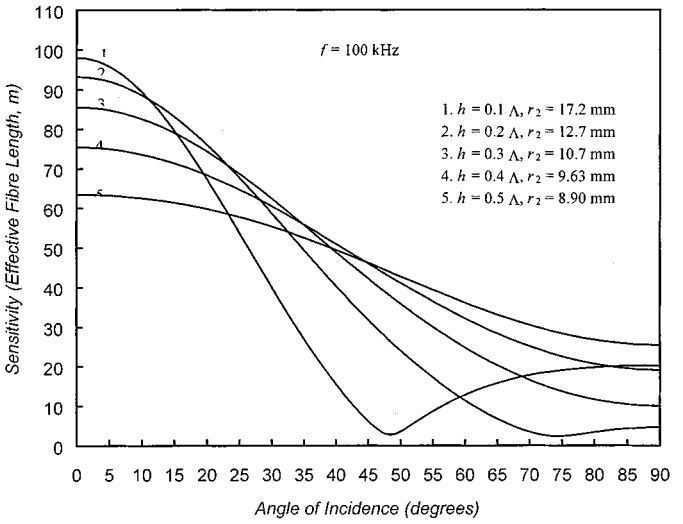

Fig. 7. Directional sensitivities for fixed fiber length and various h, with $L = 100$ m, $r_1 = 5$ mm, $f = 100$ kHz, $\Lambda = 23$ mm.

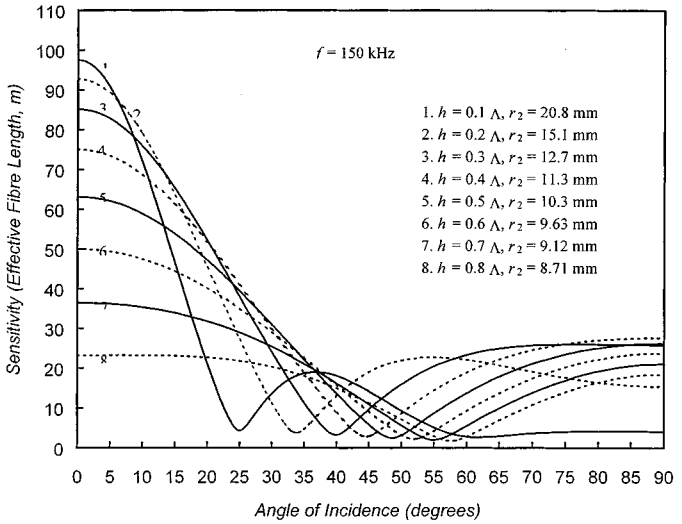

Fig. 8. Directional sensitivities for fixed fiber length and various h, with $L = 100$ m, $r_1 = 5$ mm, $f = 150$ kHz, $\Lambda = 15.3$ mm.

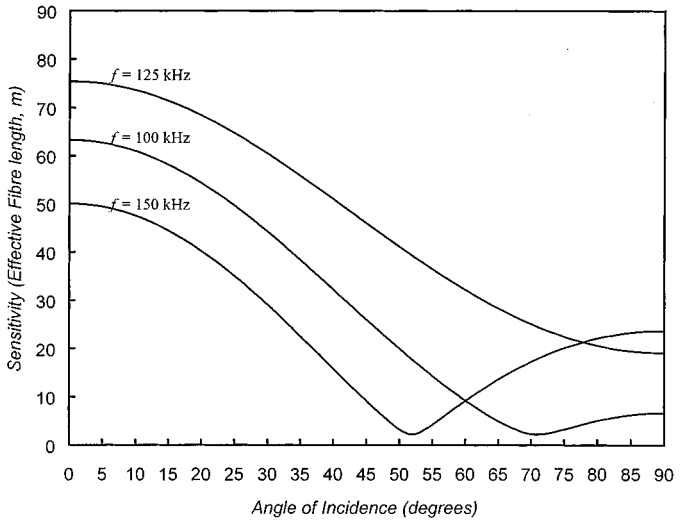

Fig. 9. Directional sensitivities of a particular fiber coil at three different frequencies, with $L = 100$ m, $r_1 = 5$ mm, $r_2 = 9.63$ mm, $h = 9.2$ mm.

In Figs. 5 and 6, the ordinates represent the quantity of $|\Delta\phi_s|/\delta\beta_0$, which has the dimension of length, so we can call this quantity the effective fiber length of the coil. The physical meaning of this quantity is that when a fiber is wound into a coil as an acoustic sensor of high frequency sound wave (short wavelength), its sensitivity is no longer equal to the sensitivity per unit length of fiber times the sensing fiber length, but depends on the coil geometry, the sound wavelength, and the incidence angle of the sound wave. Alternatively, we can regard the sensitivity of the coil to be equivalent to the sensitivity per unit length of fiber times the effective fiber length.

Figs. 7 and 8 show the effective fiber length ($|\Delta\phi_s|/\delta\beta_0$) versus the angle of orientation for a fixed fiber length $l = 100$ m, a cylinder height h varying from 0.1 Λ to 0.5 Λ for $f_a = 100$ kHz, and from 0.1 Λ to 0.8 Λ for $f_a = 150$ kHz, respectively. It is shown that for a given fiber length, the smaller the coil height h, the higher the sensitivity in the normal direction, but the narrower the directionality. It can be seen from these two figures that for a 100 kHz ultrasonic wave, if we use a 140-μm OD fiber of length 100 m, and let $h = 9.2$ mm (0.4 Λ), we can get a fairly flat directionality within 40° of incidence angle, but for 150 kHz, in order to obtain a nearly flat directionality within 40°, we need to set $h = 0.7\ \Lambda$.

The sensing coil can be designed using the calculations of directionality and the graphical analyzes presented above. Taking the fiber length $L = 100$ m, and the central sound frequency $f_a = 125$ kHz, $v_a = 2300$ m/s, and $h = 0.5\ \Lambda = 9.2$ mm, if $r_1 = 5$ mm, $d = 140\ \mu$m, then from (10) $r_2 = 9.63$ mm. For 100 kHz h is 0.4 Λ, and for 150 kHz, it is 0.6 Λ. The curves of $|\Delta\phi_s|/\delta\beta_0$ for this coil versus the angle of orientation were calculated and plotted as shown in Fig. 9. It can be seen from this figure that the directionality of this fiber coil acoustic sensor is acceptable for partial discharge detection and location.

The sensitivity of the sensor to the sound pressure ΔP can be estimated as follows. Let L' represent the effective fiber length

$|\Delta\phi_s|/\delta\beta_0$, then the induced optical phase shift of the fiber sensor is

$$\Delta\phi_s = \delta\beta_0 L' = \left(\frac{\Delta\beta}{\beta\Delta P}\right)\cdot\beta L'\Delta P$$

The quantity $(\Delta\beta/\beta\Delta P)$ is 4.9×10^{-12} for common glass fibers [5]. $\beta = 2\pi n/\lambda$, where λ is the wavelength of the light in free space and, n is the effective refractive index of the fiber. For example, for $\lambda = 830$ nm and a minimum detectable sound pressure of 0.02 Pa, which is the minimum practical sound pressure of partial discharges in oil [3], we have $\Delta\phi_s = 5.4\times10^{-5}$ rad for $L' = 50$ m. That means the demodulation circuit needs to detect a phase shift as small as 5.4×10^{-5} radians.

A calculation of the directionality of a fiber coil sensor, has been presented based on a plane wave approximation. This did not take into account the elasticity and resonance of the fiber coil as an elastic body, nor the difference in acoustic impedance of mineral oil as compared with that of the fiber coil material. Because of these effects, the acoustic wave around the coil is not a plane wave and neither is the acoustic wave inside the coil a plane wave, especially when the acoustic wavelength is comparable to the coil size. An accurate solution of this problem is not an easy task, and is beyond the scope of our present investigation.

III. Experimental Measurement of the Directionality of a Fiber Coil

In developing an acoustic sensor, its directionality must be determined. Also, through the measurement of the directionality of a specific coil sensor, we can check the accuracy of our simplified theoretical analysis. In this section, a method of measuring the directionality of the fiber coil acoustic sensor in mineral oil is presented, the experimental setup for such a measurement is described, and the results obtained for a small fiber coil in the frequency range of 50–300 kHz are given.

A. Technique for Measuring Directionality

The directionality of an acoustic sensor is the sensor's response to the acoustic waves incident upon it from various directions. Such a measurement should be carried out in a homogeneous plane-wave field, a situation which may be approximately fulfilled by a point source at sufficient distance. When directionality measurements are made in a laboratory setting, that is, in a water tank or an oil tank, the acoustic waves will be reflected by the boundaries, and the reflected waves will overlap with the direct wave, and generate standing waves. In this case, the sound field intensity will not be uniform, but be changing periodically with position. Within the frequency range of interest, the spatial period of the standing wave is about 0.5–3 cm. Since the sensor size is comparable to this, the different parts of the sensor coil will experience different sound amplitudes and affect the measurement.

To solve this problem, a gating technique was used in which the output of a sine-wave generator was gated into a series of tone bursts. A suitable delay was arranged to match the distance between the sound source and the hydrophone with the dimensions of the tank, so that the measuring gate is open only while the direct wave is being received, and is closed when the reflected wave arrives. If the time needed for the direct wave to travel from the source to the sensor is t_d, and the time needed for the first reflected wave to travel from the source to the sensor is t_r, the duration of the tone burst should be shorter than the time difference $t_r - t_d$. Because the reflection coefficient of the sound wave at the boundary of the tank is high, the reflected wave has to go back and forth several times to be attenuated to a negligible level. Therefore the time interval between the tone bursts should be long enough to achieve this attenuation.

A plastic box was used as the oil tank in these experiments. This had a length of 0.61 m, a width of 0.40 m, and was filled with mineral oil to a depth of 0.315 m. The source and the sensor were placed centrally in respect of the width and depth. The distance between the source and the sensor was 0.110 m. The distance from the sensor to the nearer end wall was 0.23 m (see Fig. 10).

Taking the velocity of sound in mineral oil as 1400 m/s, $t_d = 0.11\ \text{m}/v_a = 79\ \mu$s. In the case of the wave reflected by the tank bottom and the top liquid surface [Fig. 10(a)], the time taken by the wave to travel from the source to the sensor is $t_{r1} = 238\ \mu$s. For the wave reflected by the side walls [Fig. 10(b)], the time taken is $t_{r2} = 296\ \mu$s. For the wave reflected by the end wall near the sensor, as illustrated in Fig. 10(c), the time taken is $t_{r3} = 407\ \mu$s. Because t_{r1} is the smallest among the three values, the reflected wave that arrives first is that reflected by the bottom and the top surface. Therefore the duration of the tone burst should be less than $t_b = t_{r1} - t_d = 159\ \mu$s. This duration was therefore taken as $t_b = 150\ \mu$s.

It was found that it takes about 10 ms for the reflected waves to travel back and forth in the oil tank and attenuate to a negligible level. Thus, in the experiment, the interval between the tone bursts was taken as $t_c = 15$ ms.

B. Experimental Setup for Directionality Measurement

The setup for the directionality measurement is shown schematically in Fig. 11. The sine wave generated by the sine wave generator is gated by the gate circuit to produce a series of tone bursts. The gate circuit is driven by the pulse generator. The gate circuit includes a follower, which amplifies the signal current to drive the capacitive load of the piezoelectric transducer.

The transducer emits an ultrasonic tone burst wave, which propagates in the oil and is sensed by the fiber coil sensor. The output of the sensor demodulation circuit is measured by one channel of the digital oscilloscope, which is triggered synchronously by the pulse generator. The driving signal of the piezoelectric transducer is measured by another channel of the oscilloscope. From the display of the oscilloscope the time delay between the driving signal and the sensor output can be observed, that is, the propagation time of the ultrasonic wave from the transducer to the sensor. By properly adjusting the time scale and delay of the oscilloscope the sensor signal of the direct wave and the reflected waves of different orders are observed. The sensor is mounted on a rotatable holder, so its orientation can be changed continuously. The amplitude of the fiber sensor output

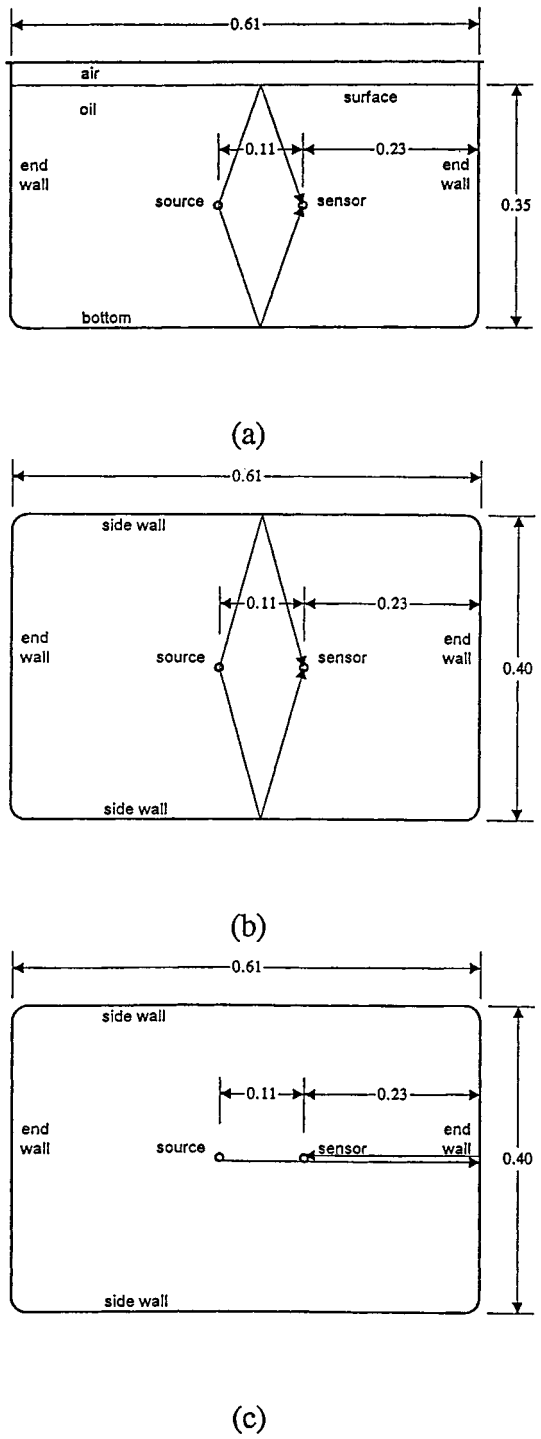

Fig. 10. Paths of the reflected waves from the source to the detector in the oil tank

was measured with the digital oscilloscope. With the driving voltage of the piezoelectric transducer kept constant at a given frequency, and the angular orientation of the sensor changed in steps, the directionality of the fiber sensor can thus be determined.

The sine wave signal generator is an ordinary laboratory signal generator with a frequency range to 1 MHz, an output amplitude to 10 V, and an output impedance of 600 Ω. The gate circuit and the pulse generator were made by using ordinary integrated circuits and other components [6]. The pulse generator was adjusted to give a pulsewidth of 150 μs, and a time interval of 15 ms [6].

The ultrasonic sound source used in the experiment was a Brüel and Kjær piezoelectric hydrophone Type 8103. This is a reverse use of the hydrophone, as suggested by the manufacturer in the Technical Documentation for the hydrophone. A typical transmitting frequency response for the hydrophone when used as a source is shown in Fig. 12 [7]. The hydrophone is 50 mm long and 9.5 mm in diameter. The acoustic center is 7 mm from the tip. The hydrophone was mounted at the end of a plastic tube 12 mm in diameter and was mounted on a plastic beam placed on top of the oil tank.

The fiber coil was fixed on a plexiglass rod, which was mounted on a plexiglass frame and could be rotated manually. A dial was fixed on the rod to indicate the orientation of the fiber coil, that is, the angle between the fiber coil axis and the line connecting the coil center and the source center.

Fig. 13 is a photograph of the experimental setup.

C. Fiber Sensor

The fiber coil used was made of bend-insensitive fiber, a single-mode fiber operating at 830 nm, with NA of 0.16, core diameter of 3.7 μm, cladding diameter of 80 μm, and coating diameter of 135 μm. The fiber length in the coil was 10.5 m. The coil was made by winding the fiber onto a paper former. UV cured optical cement was applied layer by layer as the winding was made. After the winding, the coil was cured under a UV lamp. The number of fiber turns is 274, and the number of layers is 15. The inner diameter of the coil is 11 mm, the outer diameter 14 mm, and the height 3.1 mm [8]. Using the method of Section I, the curves of $|\Delta\phi_s|/\delta\beta_0$ of this coil versus the angle of orientation are calculated and plotted as shown in Fig. 14.

The sensor is configured as a Mach–Zehnder interferometer, with the length of the reference arm equal to the sensing arm. The light source of the sensor is a single-mode diode laser operating at 830 nm wavelength, with a built-in optical isolator [8].

The effect of position errors of source and sensor on the measurement result was considered in the experiment design. The errors are mainly from the vertical position of source transducer and the sensor coil when mounted in the tank. The centers of transducer and the sensor coil should be at the same height. If they were not at the same height then, when the sensor coil axis is facing the source, or $\theta = 0$ is indicated on the dial, there will be a tilt angle α between the sensor coil axis and the line connecting the source center and the coil center. In this case the incidence angle of the sound wave to the sensor coil becomes

$$\theta' = \arccos(\cos\theta\cos\alpha)$$

instead of θ, and the minimum incidence angle is α instead of zero. This will affect the directionality curve, especially when θ is small. the position of the acoustic center of the transducer and the center of the coil was carefully set to be at the same height. In this way, the "tilt angle" is believed to have been minimized and was certainly less than 3°.

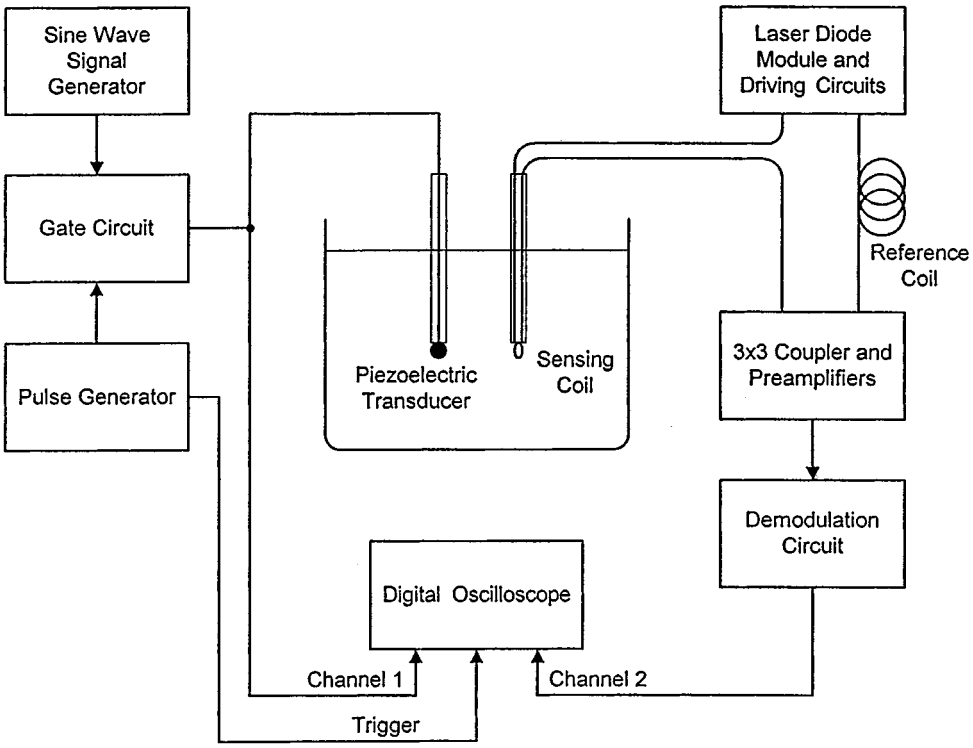

Fig. 11. Experimental setup for the directionality measurements

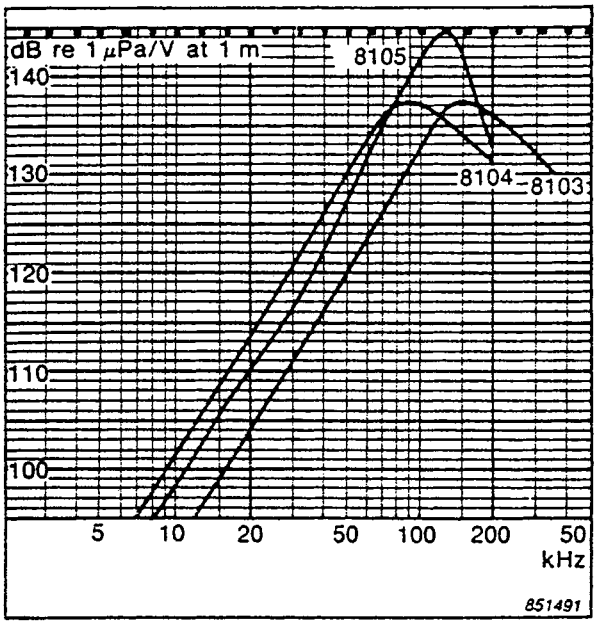

Fig. 12. Typical dB/voltage transfer function of the B&K Type 8013 (and others) when used as ultrasonic sound sources.

D. Demodulation Scheme

The demodulation scheme is a passive homodyne with a 3×3 coupler [9]. The demodulation circuit adopted for the directionality measurement was the improved symmetric circuit described in [10]. Two manually adjusted polarization controllers were inserted into the sensing arm and the reference arm respectively. The amplitude of one of the preamplifier outputs and the waveform of the square sum signal were monitored with an oscilloscope. In the measurement, the states of polarization of the two arms were adjusted to keep the output of the preamplifier at maximum and the square sum signal to be constant. When these two conditions are fulfilled, the working of the demodulation circuit is optimized.

E. Experimental Result of Directionality Measurement

The experimental results of the directionality measurements are plotted in Fig. 15(a)–(d). The curves shown in Fig. 15(a) and (b) are polynomial best-fit curves. The curves shown in Fig. 15(c) and (d) are not from the polynomial fitting, but are just curves connecting the actual measurement points, because the experimental data of the measurements at these high frequencies are too complicated to be fitted to polynomial functions.

The amplitude of the driving voltage was kept constant during the measurements at each frequency. However, the frequency responses of both the piezoelectric hydrophone source and the fiber optic sensor are not flat. There are some resonance frequencies in the transducer-sensor system within the range 50–300 kHz. In order to obtain good accuracy, the detected signal should have enough amplitude to give a high signal-to-noise ratio (SNR). Therefore, the amplitude of the driving voltage was increased at the higher frequencies to compensate for the lower frequency response of the transducer, as shown in Table I. At the frequencies of 60 and 70 kHz, because of a resonance of the fiber coil at a frequency between them, the amplitude of the received signal was too high for a normal driving voltage of 1 V, so the amplitude of the driving

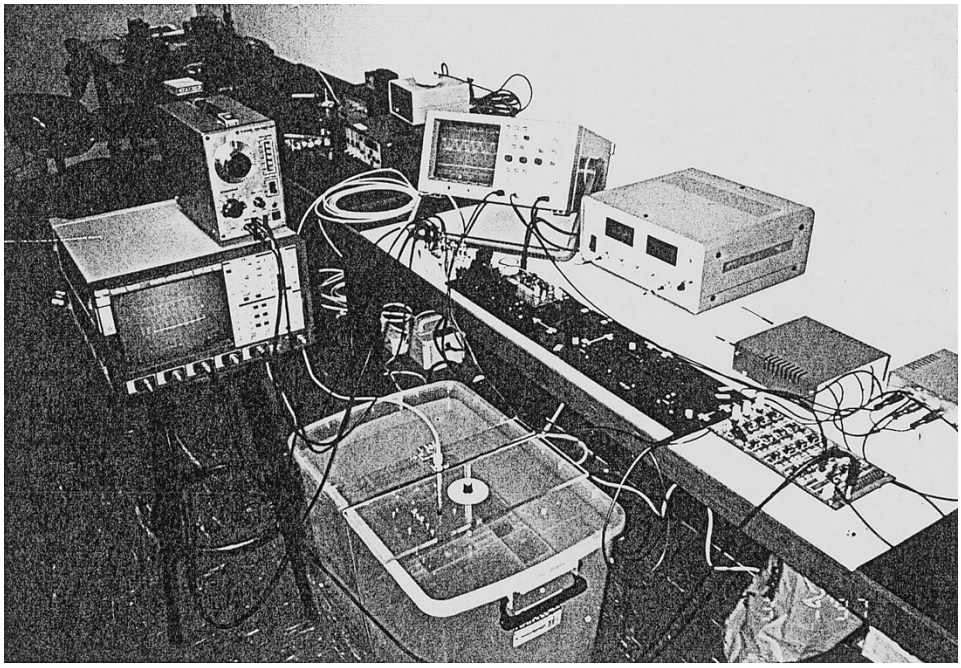

Fig. 13. The experimental setup for the directionality measurements.

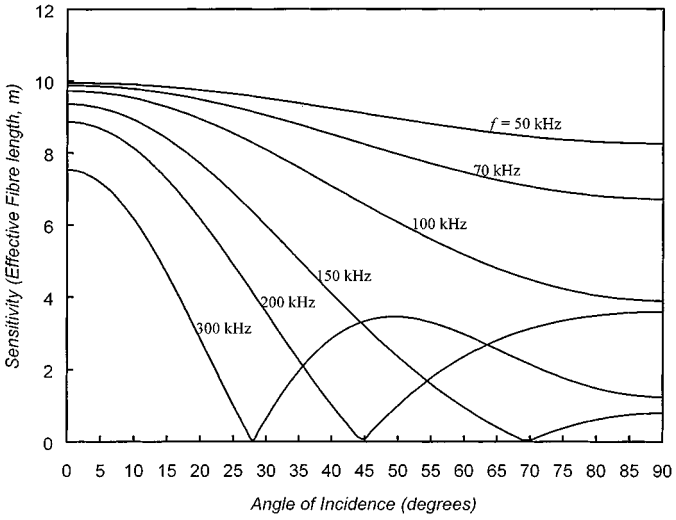

Fig. 14. Directional sensitivities of a small fiber coil at various frequencies, with $L = 10.5$ m, $r_1 = 5.5$ mm, $r_2 = 7.0$ mm, $h = 3.1$ mm, $v_a = 2300$ m/s.

voltage was reduced, in order to make the readings at these two frequencies comparable to the others.

IV. Discussion

The experimental results of the directionality measurement are not in close accordance with the results of the calculation given in Fig. 14, as well as in Figs. 3–9. In the theoretical results, the directionality curves always have their maximums at 0° incidence angle, while the experimental curves mostly have the maximums at other angles, although some of them have a peak at 0°. For higher frequencies, the positions of the peaks and the valleys on the theoretical curves and the experimental curves are also different.

In Fig. 14, the sound velocity was taken as 2300 m/s, which is the mean value for the longitudinal sound velocity in the fiber coil, using typical material parameters for the complex composite structure [5]. Comparing Fig. 14 with Fig. 15(c) and (d), we find there is a correspondence for the position of the minimum at $f = 150$ kHz, but for the higher frequencies, the numbers of peaks and valleys do not correspond. If we use the sound velocity in the oil for this calculation, $v_a = 1400$ m/s, we obtain the results as shown in Fig. 16. Comparing Fig. 16 with Fig. 15(c) and (d), we found the numbers of peaks and valleys correspond, but the positions of them are not the same on the theoretical and experimental curves. These comparisons reveal that neither of these sound velocities may be properly used in the calculation. For the choice of v_a the oil and the coil material should both be considered.

Now if we use a velocity in between these two velocities, such as $v_a = 1800$ m/s, for the calculation, the results shown in Fig. 17 are obtained. Comparing Fig. 17 with Fig. 15(c) and (d), both the numbers and positions of the peaks and valleys correspond roughly to those for 200 and 300 kHz.

The resonance of the fiber coil is apparent from the experimental results shown in Fig. 15(a)–(d) and Table I. The resonant frequencies are at about 60 and 240 kHz. This effect is not predicted by the simplified theoretical model.

The experimental results show that the directionality of the fiber coil is quite complicated, and cannot be calculated exactly by the simple plane wave model, at least not for the frequency range of interest, from 50–300 kHz. The reasons why this simple, conventional theory is insufficiently accurate were considered in Section II: that it appears the discrepancy may be due to an elastic effect which is not taken into account in the theoretical model. A more accurate theoretical model needs to be established. It is also seen that the maxima and minima only

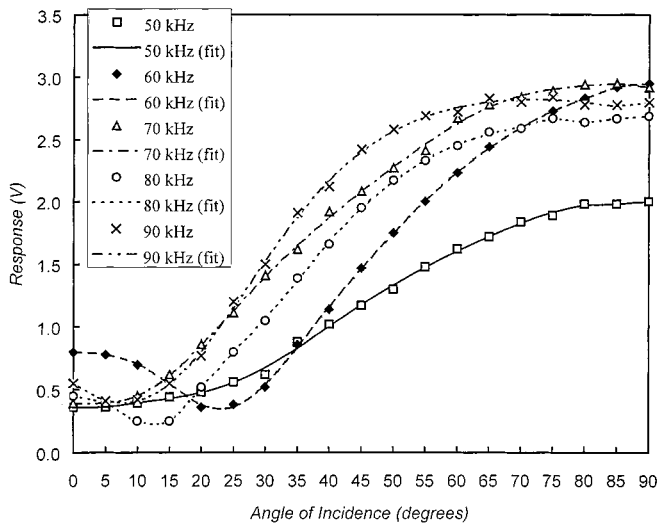

(a)

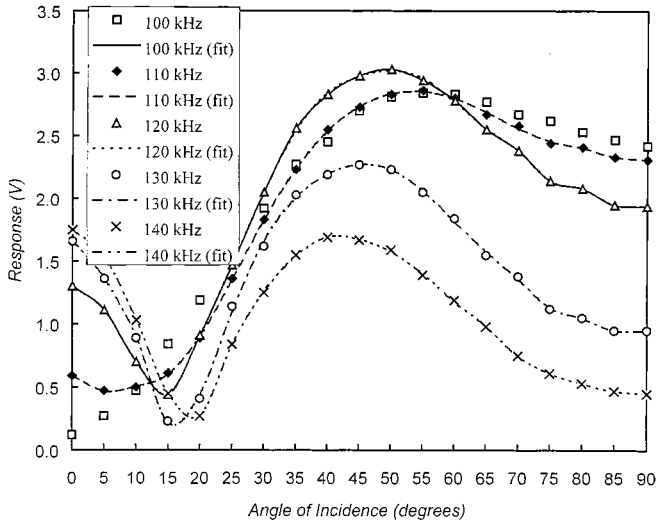

(b)

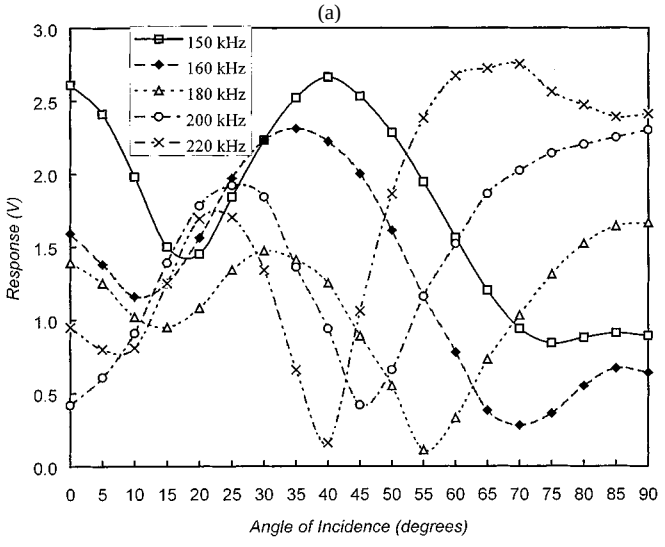

(c)

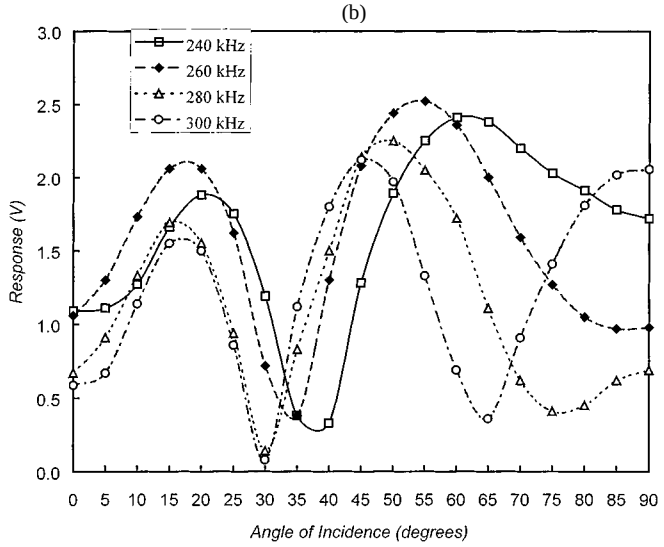

(d)

Fig. 15. (a) Directional sensitivities for the frequencies 50 , 60, 70, 80, and 90 kHz, (b) 100, 110, 120, 130, and 140 kHz, (c) 150, 160, 180, 200, and 220 kHz, and (d) 240, 260, 280, and 300 kHz.

TABLE I
AMPLITUDE OF THE APPLIED TONE BURST SIGNAL AT VARIOUS FREQUENCIES IN ORDER TO PROVIDE SIMILAR OUTPUT AMPLITUDE FROM THE DETECTION CIRCUITS

Frequency	50 kHz	60 kHz	70 kHz	80 kHz	90 kHz	100 kHz	110 kHz	120 kHz	130 kHz	140 kHz
Driving Amplitude	1.0 V	0.5 V	0.7 V	1.0 V	1.0 V	1.0 V	1.0 V	1.0 V	1.0 V	1.0 V
Frequency	150 kHz	160 kHz	180 kHz	200 kHz	220 kHz	240 kHz	260 kHz	280 kHz	300 kHz	
Driving Amplitude	2.0 V	2.0 V	2.0 V	2.0 V	1.25 V	1.0 V	1.5 V	2.0 V	3.0 V	

correspond if a compromise value of sound velocity is used, between those for the oil and the coil materials.

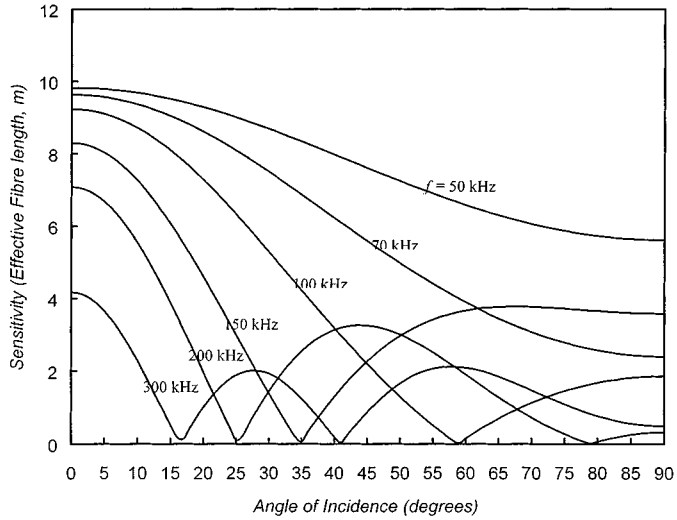

Fig. 16. Directional sensitivities of a small fiber coil at various frequencies, with $L = 10.5$ m, $r_1 = 5.5$ mm, $r_2 = 7.0$ mm, $h = 3.1$ mm, $v_a = 1400$ m/s.

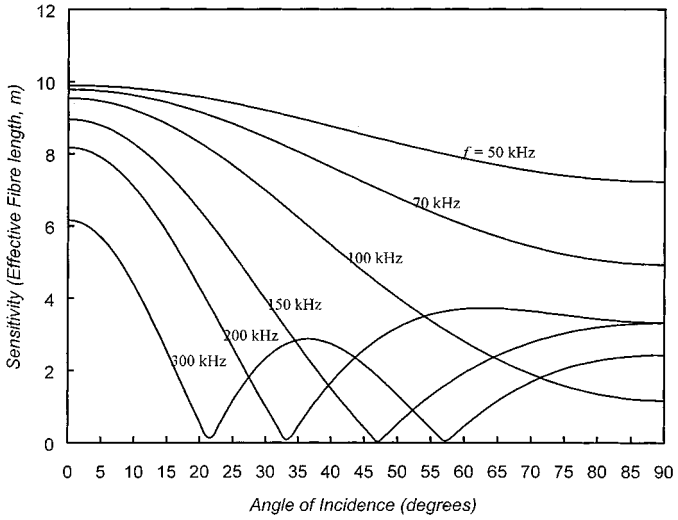

Fig. 17. Directional sensitivities of a small fiber coil at various frequencies, with $L = 10.5$ m, $r_1 = 5.5$ mm, $r_2 = 7.0$ mm, $h = 3.1$ mm, $v_a = 1800$ m/s

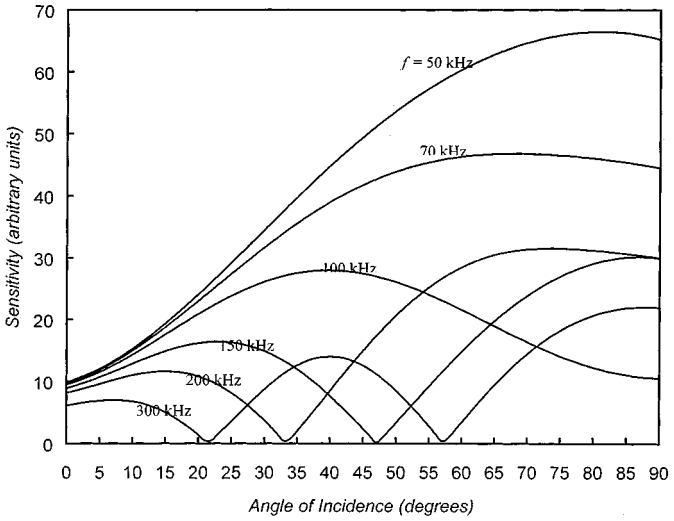

Fig. 19. Directional sensitivities of a small fiber coil at various frequencies (Modified by an exciting factor as a function of incidence angle), with $L = 10.5$ m, $r_1 = 5.5$ mm, $r_2 = 7.0$ mm, $h = 3.1$ mm, $v_a = 1800$ m/s.

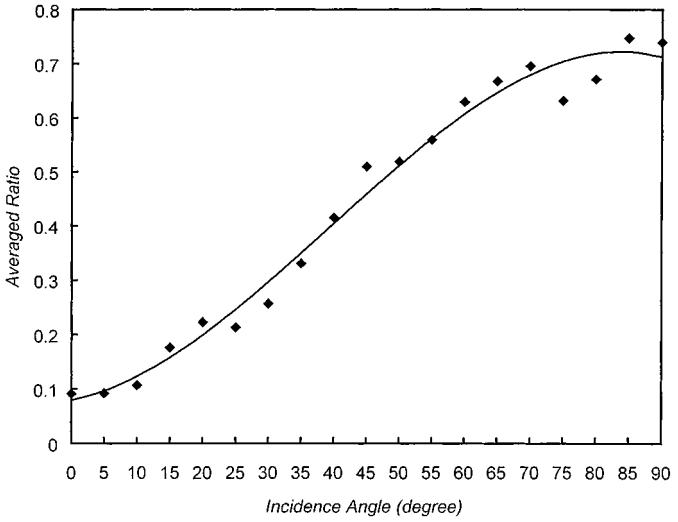

Fig. 18. Averaged ratio of experimental to calculated directional sensitivities of the small fiber coil, with $L = 10.5$ m, $r_1 = 5.5$ mm, $r_2 = 7.0$ mm, $h = 3.1$ mm, $v_a = 1800$ m/s.

From the experimental results it may be seen that for all frequencies there is a trend whereby the ratio of the experimental response of the sensor to the calculated response increases with increase in the incidence angle.

The ratio is plotted in Fig. 18 as an average for all frequencies, using the compromise velocity, 1800 m/s. (The different exciting voltages of Table I were taken into consideration). Using this "angle sensitivity factor," averaged from measurements at all frequencies, the directionality may be re-calculated: the results are shown in Fig. 19. This corresponds reasonably well to the observed directionality.

From the experimental results, we can see that although the fiber coil acoustic sensor has complicated directionality patterns, it does have a good acoustic response and an acceptable directionality in the frequency range of our interest. Therefore, the fiber coil sensor can be a good tool for application to the acoustic detection and location of partial discharges.

In future work, it is hoped to develop an improved, but very much more complex, calculation which can take into account the differing sound velocities in oil and coil sensor; the sensitivity resonances; and the directional sensitivity whereby it is so much more sensitive at 90° than 0°, whatever the frequency. Nevertheless, the measurements are internally consistent (as evidenced by Figs. 18 and 19); and the maxima and minima will tend to be averaged out in practice since the sensor will be responding to the partial discharge pressure pulses, which comprise a range of frequencies. It is likely, therefore, that it will in practice give a satisfactory response to partial discharges and enable their detection and location.

V. Conclusion

A calculation of the directionality of a fiber coil acoustic sensor has been made by using a plane wave approximation method. The results show that if the diameter of a fiber coil sensor is less than 20 mm, its directionality is relatively flat within 40° for frequencies below 150 kHz. Such directionality is acceptable for the application of partial discharge location in oil-filled high-voltage transformers.

The directionality of a fiber coil acoustic sensor has been measured by using the gating technique for frequencies from 50 to 300 kHz. The results show that the directionality of the fiber coil is not wholly consistent with those obtained in the calculations. The discrepancies are likely to originate in elastic resonances not considered in the simplified model, as well as the different sound velocities within the oil and the coil sensor. Further investigation into these problems will be the object of future work.

Nevertheless, the experimental results indicate that the fiber coil sensor and the detection circuits developed in this work can successfully be applied to the detection of partial discharges in power transformers.

REFERENCES

[1] L. E. Lundgaard, "Partial discharge—Part XIV: Acoustic partial discharge detection—Practical application," *IEEE Elect. Instrum. Mag.*, vol. 8, pp. 34–43, 1992.

[2] T. R. Blackburn, B. T. Phung, and R. E. James, "Optical fiber sensor for partial discharge detection and location in high-voltage power transformer," in *Proc.IEE 6th Int. Conf. Dielect. Mater., Measure. Appl.*, Manchester, U.K., 1992, IEE Conf. Pub. 363, pp. 33–36.

[3] Z. Zhao, M. S. Demokan, and J. M. K. MacAlpine, "Optic fiber acoustic sensor for sensing and locating partial discharges in high voltage oil-filled power transformers," in *Proc. 21st Australian Conf. Optic. Fiber Tech.*, Queensland, Australia, Dec. 1996, pp. 286–289.

[4] N. Lagakos and J. A. Bucaro, "Linearly configured embedded fiber-optic acoustic sensor," *J. Lightwave Technol.*, vol. 11, pp. 639–642, 1993.

[5] S. Knudsen and K. Bløtekjær, "An ultrasonic fiber-optic hydrophone incorporating a push-pull transducer in a Sagnac interferometer," *J. Lightwave Technol.*, vol. 12, pp. 1696–1700, 1994.

[6] Z. Zhao, "Fiber optic acoustic sensing and locating of partial discharges in high-voltage oil-filled power transformers," Ph.D. dissertation, The Hong Kong Polytechnic Univ., 1998.

[7] "The graph is from the technical documentation for Brüel & Kjær hydrophones types 8103, 8104, 8105, and 8106,", Revision, Mar. 1992.

[8] Z. Zhao, M. S. Demokan, and J. M. K. MacAlpine, "Development of an optical fiber acoustic sensor for sensing and locating partial discharges in high voltage oil-filled transformers," IEEE Trans. Instrum. Measure., submitted for publication.

[9] D. A. Brown, C. B. Cameron, R. M. Keolian, D. L. Gardner, and S. L. Garrett, "A symmetric 3×3 coupler based demodulater for fiber optic interferometric sensors," in *Fiber Optic Laser Sensors IX*: SPIE, 1991, vol. 1584, pp. 328–335.

[10] Z. Zhao, M. S. Demokan, and J. M. K. MacAlpine, "Improved demodulation scheme for fiber optic interferometers using an asymmetric 3×3 coupler," *J. Lightwave Technol.*, vol. 15, pp. 2059–2068, 1997.

Zhao Zhiqiang received the B.Sc. degree in physics from the Tsinghua University, China, in 1982 and the M.Sc. degree in physics from the Institute of High Energy Physics, Chinese Academy of Sciences, China, in 1985. He received the Ph.D. degree in electrical engineering from The Hong Kong Polytechnic University in 1999.

He worked in the Institute of High Energy Physics on gravitational physics experiments from 1985 to 1992. He was a Research Assistant in the Department of Manufacturing Engineering of The Hong Kong Polytechnic University in 1993, involved in a research project on fiber optic sensor applications in robots. He was a Research Assistant and a Ph.D. candidate in the Department of Electrical Engineering of The Hong Kong Polytechnic University from 1994 to 1997, studying optical fiber acoustic sensing and locating of partial discharges in oil-filled high voltage transformers. He then worked as an Engineer on fiber-optic communication networks in Singapore from 1997 to 1999. Now he is a Lecturer at the Temasek Polytechnic in Singapore.

Mark MacAlpine received the B.A. and M.A. degrees in physics from Cambridge University, Cambridge, U.K., and the Ph.D. degree in electrical engineering at Queen Mary College, London University, London, U.K., in 1963, 1964, and 1968, respectively.

He has been with the Hong Kong Polytechnic, now the Hong Kong Polytechnic University, Hong Kong, China, for 25 years and is currently an Associate Professor and the Associate Head of the Electrical Engineering Department. Before coming to Hong Kong he worked in applied research with the United Kingdom's Central Electricity Generating Board, in teaching with the HSI University in Ethiopia, and in quality assurance with International Computers Limited, U.K. His research interests lie principally in high-voltage insulation studies but also in applications of electrical engineering in the textile industry and in teaching and learning methods.

Dr. MacAlpine is a member of the Hong Kong Institution of Engineers and a member of the Institution of Electrical Engineers (IEE).

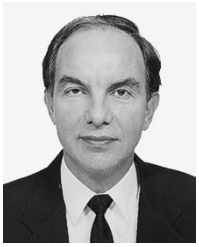

M. Süleyman Demokan (SM'89) received the B.Sc. degree in electronic engineering from the Middle East Technical University, Turkey, in 1970 and the M.Sc. and Ph.D. degrees, also in electronic engineering, from King's College, University of London, London, U.K., in 1972 and 1976, respectively.

He served in the Middle East Technical University in various capacities, including Dean of Faculty, Head of Department and Associate Professor, between 1976 and 1983. After conducting research for a year at Imperial College (University of London) as a Visiting Senior Research Fellow, he joined the Hirst Research Center of the General Electric Company, U.K., in 1984, where he directed contract research as Head of Department (Optoelectronic Components) and Chief Scientist (Optical Communications). Since 1988 he has been with The Hong Kong Polytechnic University, first as the Head of the Department of Electrical Engineering and, from 1995, as the Dean of the Faculty of Engineering. In 1992, he was conferred the title of Chair Professor of Electrical Engineering. Since 1997, he has also assumed responsibility as an Associate Vice-President of the University. His current research interests include optical communication systems and fiber-optic sensors.

Dr. Demokan is a Fellow of the Hong Kong Institution of Engineers and a Fellow of the Institution of Electrical Engineers (IEE).